Rejuvenation Addresses Partial Discharge in Power Cables

Glen J. Bertini
Novinium, Inc.
22820 Russell RD,
Kent, WA, USA

Hunly Chy
Southern California Edison
1 Innovation Way
Pomona, CA, USA

ABSTRACT

Rejuvenation of power cables addresses water trees, voids, or electrical trees. Partial discharge (PD) in joints or terminations are addressed by the sustained pressure rejuvenation process, which replaces all terminations and joints. In this study, partial discharge inception voltage (PDIV) is found to increase by 27% for each 0.1%w increase in fluid concentration in field-aged rejuvenated cable samples. The mechanism of rejuvenation is discussed in which PD mechanism is prevented by plasticizing the dielectric, filling the voids, smoothing electrical stress, and sequestering free electrons in field-aged cables.

Index Terms — **AC breakdown, cable rejuvenation, maximum partial discharge magnitude at breakdown, partial discharge inception voltage, PDIV**

1 INTRODUCTION

WELL established by [1] and elsewhere, the root cause of most failures of medium voltage solid dielectric cable is water treeing and related phenomena. Early rejuvenation fluid development effort focused on reversing the dielectric damage of water trees and retarding their growth. Dozens of contributions, including [2–4], demonstrate cable rejuvenation accomplishing these goals. Over the course of 35 years, practical results have demonstrated multidecade life extension of rejuvenated cables. The contributions of [5, 6] presented a theoretical basis of how modern rejuvenation fluids address partial discharge (PD) in gas-filled voids including electrical trees. In this contribution, the author and his colleagues employed continuous partial discharge monitoring according to the IEC 60270 standard, while samples were being subjected to AC breakdown testing. For the first time, the relationship between PD characteristics and AC breakdown (ACBD) performance were able to be correlated. Further, micro infrared spectroscopy was employed to determine the concentration of rejuvenation fluid in field-aged cable samples allowing the correlation of rejuvenation concentration with PD and ACBD.

1.1 PARTIAL DISCHARGE MECHANISM

Figure 1, adapted from [6], summarizes the elements that lead to PD in gas-filled voids and the mechanisms by which rejuvenation interferes with those elements. Partial discharge mechanisms are summarized in [7, 8]. In brief, PD requires four elements:

Element 1. There must be a free electron, most likely from the collision of a cosmic ray with a gas molecule.

Element 2. The free electron must be in a gas-filled void. Liquid-filled voids do not suffer PD.

Element 3. The gas-filled void must be of sufficient length, parallel to the electrical field gradient.

Element 4. The electrical field must be strong enough to accelerate a free electron to a threshold energy required to initiate an electron avalanche.

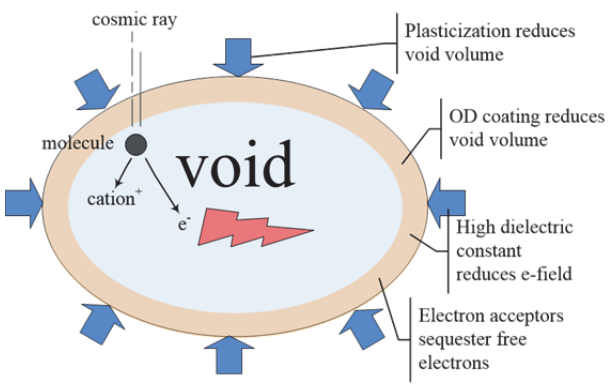

Figure 1. PD mechanisms and how rejuvenation addresses them.

Manuscript received on 13 August 2020, in final form 18 September 2020, accepted 18 September 2020. Corresponding author: G. J. Bertini.

DOI: 10.1109/TDEI.2020.009286

1.2 HOW REJUVENATION ADDRESSES PARTIAL DISCHARGE

Four mechanisms were proposed in [5–6] to explain how modern fluid rejuvenation technology interferes with the four required elements for partial discharge inception and propagation described in Section 1.1.

Mechanism 1. Silanes and siloxanes occupy the intermolecular spaces between solid dielectric polymer molecules. These materials plasticize and swell the polymer. The swelling polymer must expand somewhere, and, hence, gas-filled voids are reduced in size as they are mechanically compressed. The reduction in gas-filled void volume reduces the probability of the cosmic ray interaction – mitigating element 1. The gas-filled void length is shortened – mitigating element 3. Comonomer tolylethylmethyldimethoxysilane is commonly utilized for optimum plasticization. An increase in the concentration of siloxanes inducing polymer swell has been shown in [5, 9] to increase dielectric performance.

Mechanism 2. The surface energy of modern rejuvenation , as shown by [10], is lower (about 20 dyne/cm) than that of the solid dielectric polymer (about 30 dyne/cm). Rejuvenation fluids remain liquid for their lifetimes as they co-oligomerize. The low surface energy encourages the fluid to accumulate on the surfaces of the relatively higher surface energy solid polymer surfaces. As described in [5, 6], the fluids coat the inner surface of gas-filled voids, thus reducing their outside diameter (OD) and total gas-filled void volume. Depending on the local concentration of fluids and void geometry, smaller voids may be filled entirely; larger voids will be partially filled, reducing gas-filled void volume. Like mechanism 1, the reduction in gas-filled void volume reduces the probability of the cosmic ray interaction – mitigating element 1. The gas-filled void length is shortened – mitigating element 3. Additionally, at least a portion of the void is liquid filled and cannot support PD – mitigating element 2. Comonomer tolylethylmethyldimethoxysilane is commonly used to minimize surface energy.

Mechanism 3. Modern rejuvenation fluids include co-monomers with dielectric constants greater than that of water. Analogous to how high dielectric constant materials grade stress at cable terminations on a macro scale, the inclusion of high dielectric constant fluid on the inner surface of voids grades and dampens electrical stress within the remaining gas-filled void volume at nano to micro scales – mitigating element 4. Cyanobutylmethyldimethoxysilane is commonly used to create a high dielectric constant co-oligomer.

Mechanism 4. Modern rejuvenation fluids include several electron acceptors or voltage stabilizers, which have been shown by [11–15] to sequester free electrons – mitigating element 1. Combinations of phenolic antioxidants, hindered amine light stabilizers or HALS, and metallocene compounds are employed in modern rejuvenation fluids as electron acceptors.

In short, modern rejuvenation fluids are designed to mitigate all four elements required for partial discharge initiation in a cable. In this contribution, the authors explore the efficacy of this approach in field-aged cables.

1.3 AC BREAKDOWN VS. CONCENTRATION OF LEGACY REJUVENATION

Figure 2 provides a summary view of [4, 9, 16], which together demonstrate the relationship between post-rejuvenation ACBD and the average concentration of legacy fluid (coded '841) in cable insulation. Equation (1) defines a transformation of post-rejuvenation ACBD.

$$\Delta ACBD = \frac{ACBD_{treated} - ACBD_{control}}{ACBD_{new} - ACBD_{control}} \quad (1)$$

This transformation normalizes post-rejuvenation results to an increase in ACBD performance where the denominator is an estimate of dielectric strength lost over a cable's service life. Thus a 100% ΔACBD indicates that all dielectric strength lost has been recovered. To utilize the Equation (1) transformation, it is almost always necessary to assume a value for $ACBD_{new}$. For PE cables, a value of 39.37 kV/mm is assumed. If that assumption is uniformly applied, any error in the assumption is of low consequence when any two ΔACBD results are compared. $ACBD_{control}$ is an estimate of the cable sample's ACBD before treatment. Since ACBD is inherently destructive, this value cannot be determined directly. Instead, similar untreated control samples are sacrificed to generate this estimate. Where at least one control subsample is available from the identical cable sample, the arithmetic average of any values is used to make this estimate. Of the 25 ACBD values, 19 enjoyed a direct comparison to at least one control. For the remaining 6 samples, the $ACBD_{control}$ was the overall average of all control samples. Errors in this value are mitigated as the term appears in both the numerator and denominator. However, a high estimate for this value can lead to negative ΔACBD values for modest rejuvenation fluid concentrations. Actual negative values are unlikely absent an estimation error.

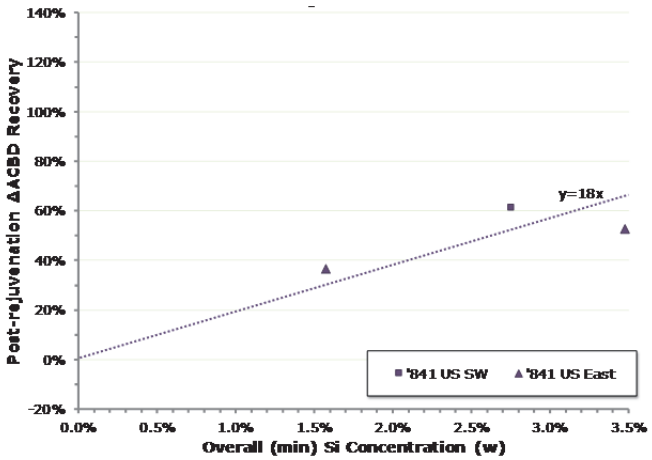

Figure 2. Legacy fluids utilized in the 20th Century experience about an 18% change in ACBD recovery for each 1% increase in rejuvenation fluid concentration.

The transformation provided by Equation (1) fits the generalized linear model (GLM), described in Section 3.1, considerably better than raw data expressed either as absolute values ($ACBD_{treated}$) or perturbations from the absolute value

from the control ($ACBD_{treated}$ – $ACBD_{control}$). The models' Akaile's Information Criterion or "AIC" values are about -6.1 and 319 with and without transformation, respectively. The preferred model enjoys the minimum AIC value.

The more defects a cable sample harbors, the greater the impact a given concentration of fluid imparts upon the sample. For example, in [17] new cable treated with phenylmethyldimethoxysilane together with 0.2%$_w$ titanium (IV) isopropoxide catalyst and, subsequently, laboratory aged at 2.5U_0 in water for six months experienced about a 44% increase in ACBD (i.e., the quotient of 47.2 and 38.4 kV/mm) compared to the untreated control. Applying Equation (1), its ΔACBD is 293% (i.e., the quotient of 47.2–32.7 and 38.4–33.5). After 6 months of accelerated aging, the dielectric strength gained by treating a new cable was almost three times more than the loss of dielectric strength in the untreated control. The transformed result correlates better with fluid concentration in other studies and provides a more meaningful comparison to new cable. A 100% ΔACBD approximates a like-new condition.

1.4 WEAKEST LINKS

A corollary for the adage, "A chain fails at its weakest link," is "A cable fails at its longest water tree." In [1] this corollary was demonstrated. Consider the blue line in Figure 3, which is a hypothetical ACBD strength for each 1 m portion of a 100 m cable, were it possible to make such measurements. In this example, the largest water tree is located at 33 m and without treatment the cable will likely fail when the voltage exceeds about 8 kV/mm at 33 m. The introduction of rejuvenation fluid increases the ACBD voltage across the cable, as illustrated by the hypothetical orange line. The failure location is changed from the 33 m mark to 39 m. Fluid concentration is not uniform along the cable axis or its radial orientation. We examine fluid distribution in more detail in Section 2.2 "Concentration Considerations."

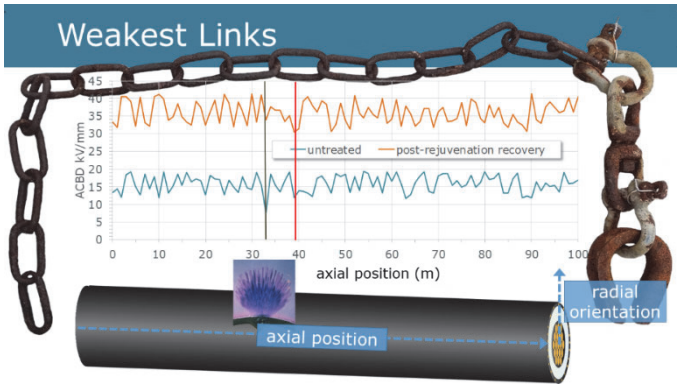

Figure 3. Post-rejuvenation ACBD is a function of two independently stochastic values. Dielectric defects are distributed randomly in a cable and rejuvenation fluid concentration profiles are not uniform. In this hypothetical example, the largest water tree is at 33 m and were the cable not treated it would fail there, but the increase in ACBD provided by treatment is quasi-random and the treated cable fails at a value over 300% higher than the untreated cable and at 39 m.

The stochastic natures of water treeing and fluid concentration suggest that the best insights to long-term life-extension shall be determined at local low concentration. The weakest link is determined by the conflation of the locations of defects in a cable and of the locations where fluid concentration is lower. Over the course of decades in post-treatment service, the fluid concentration in treated cables decreases as fluid permeates through the insulation. The most efficacious rejuvenation fluid – the one that provides the best dielectric properties for the greatest length of time – is rejuvenation fluid that is effective at low concentration. In Section 2, concentrations 3 to 7 times lower than those represented in Figure 2 are examined.

2 METHODS AND PROCEDURES

2.1 CABLE SAMPLES

Fifteen residential distribution cable lengths of 12–120 m of 33.6 mm^2 aluminum conductor 5.6 mm nominal XLPE insulation in conduit were pulled after some decades in service. An unaffiliated third-party off-line partial discharge testing firm had designated each cable as "critical." That is, failure was deemed imminent. The testing firm recommended immediate replacement. Table 1 provides a summary of these 19 cable segments. Each segment was subdivided into samples about 12 meters in length yielding 126 samples. The remaining samples were randomly assigned to one of four groups. Eight samples were untreated controls. Twenty-five samples were treated with 25 different unit fluid quantities and three post-treatment aging regimens designated as T7, T30, and T90 to yield a variety of modest fluid concentration profiles.

Table 1. Sample designations by length. Manufacturing vintage and at least five manufacturers (Mfr. Coded 0-5, where 0 indicates unknown) are represented. Sampling was distributed and randomized. Samples are coded as follows: Black signifies control; grey signifies treated cohorts, where dark grey (T7), medium grey (T30) and light grey with black characters (T90) were treated with modest and different amounts of rejuvenation fluid and aged for 7, 30 or 90 days, respectively, in water at 55°C; white were unused. Samples delineated with the Greek character "μ" included fluid concentration profiles obtained by μFTIR. Boxes with white diagonal lines suffered transportation damage discussed in Section 3.2.

		length (m)								
Vintage	Mfr.	12	24	36	48	60	72	84	96	108	120
1972	2	6	7								
1972	3	11	12	13	14	15	T30-16μ	T30-17μ	18		
1987	4	T30-19μ	20	21	22	23					
1977	0	27	28	29							
1979	5	30	31	C-32	T90-33μ	T30-34μ	35	T30-36μ	C-37	38	
1984	5	40	T90-41μ	T7-42μ	C-43	C-44	T30-45μ	T7-46μ	T30-47μ		
1972	2	58	59	60	61	62	63	64	T90-65μ	T7-66	
1972	2	T7-67μ	68	69	70	71	T30-72μ	T90-73μ	74	T90-75μ	
1994	4	T7-84μ	85	T90-86μ	C-87	88	T30-89μ	90	91		
1969	0	116	T90-117μ								
1979	5	C-118	T90-119μ								
1972	2	T7-120μ	C-121								
1977	0	122									
1970	0	C-123									
1977	0	124	T7-125	T7-126μ							

Following the completion of electrical testing, approximately 20 wafers were examined by optical microscopic for the control, T7, T30, and T90 sample groups. Each wafer was taken at a random location distant from the breakdown site. Voids, water tree counts, and tree length distributions were cataloged and summarized in Table 2.

Additionally, wafers at each cable breakdown site were also similarly examined. Most failure paths originated at the inner or outer semi-conductive screens suggesting that vented water trees or defects at those interfaces may have originated the

breakdowns. Four sample fault channels, namely C-121, C-123, T30-34 and T90-117, had large co-located vented water trees. The remaining failure channels had no identifiable defects – perhaps erased by the breakdown energy.

There was nothing extraordinary in these observations. The cable samples were generally in conditions that would be expected of their respective vintages and service life.

Table 2. Void and water tree quantification for select cable samples.

	Bow-Tie Trees		Inside Vented Trees		Outside Vented Trees		Voids
Cable	Density <25%	Count >25%	Density <25%	Count >25%	Density <25%	Count >25%	Count >.051mm
C-37	0.079	1	0.0040	0	0.0006	0	0.0046
C-118	0.071	2	0.0034	0	0.0010	0	0.0020
C-123	0.015	0	0.0012	0	0.0012	0	0.0026
T7-66	0.001	0	0.0004	0	0.0029	0	0.0000
T7-67	0.002	0	0.0002	0	0.0006	0	0.0002
T7-120	0.001	0	0.0000	1	0.0006	0	0.0000
T30-17	0.081	0	0.0434	3	0.0016	0	0.0049
T30-34	0.036	1	0.0008	0	0.0000	0	0.0008
T30-36	0.088	1	0.0037	1	0.0004	0	0.0008
T90-33	0.043	0	0.0008	0	0.0002	0	0.0008
T90-65	0.006	0	0.0003	0	0.0002	0	0.0004
T90-73	0.009	0	0.0006	0	0.0004	0	0.0013

2.2 CONCENTRATION CONSIDERATIONS

In [4, 16] the relationship between AC breakdown and vintage rejuvenation fluid has been thoroughly demonstrated. Treatment concentrations on recently rejuvenated cables can reach more than 3%$_w$. At these concentrations of several weight percent, the AC breakdown strength is generally more than 40 kV/mm, a value typical of new cable, and the probability of failure in service is virtually nil. This contribution focuses on average concentration below about 0.5%$_w$. One-half weight percent is about 14–33% of typical post-rejuvenation fluid concentrations, illustrated in Figure 2.

Sample cables were analyzed with microscopic Fourier transform infrared spectrometry (μFTIR) to determine the concentration profile within the insulation along its approximately 5 mm radius beginning at the conductor-shield/insulation interface and ending at the insulation/insulation-shield interface. Spectrometry was generally applied at 0.25 mm steps. Figure 4 shows a family of exemplary μFTIR traces for the 22 steps across a cable sample insulation radius. While there are perturbations along the entire measured infrared range spanning 2000 to 600 cm^{-1}, our focus is on two absorption bands centered near 1303 cm^{-1} and 1258 cm^{-1}. The former is the absorption band for PE; the latter is the absorption band for the silicon-carbon bond (Si-C). The ratio of the integrals of these two absorbance peaks is proportional to the silicone concentration in PE.

Gravimetric calibration determines the required proportionality constant. A plaque of PE is accurately weighed, immersed in rejuvenation fluid monomer for various times and at various temperatures, weighed again to determine the increase in mass from the rejuvenation fluid and immediately subjected to FTIR. The calibration constant is determined by the application of Beer's Law and fitting an absorbance line through the origin and the data by least squares. The calibration is illustrated in Figure 5 and yields a formula of y = 0.0774x, where y is the fractional mass gain and x is the ratio of the integral of the silicon-carbon peak to that of the PE peak.

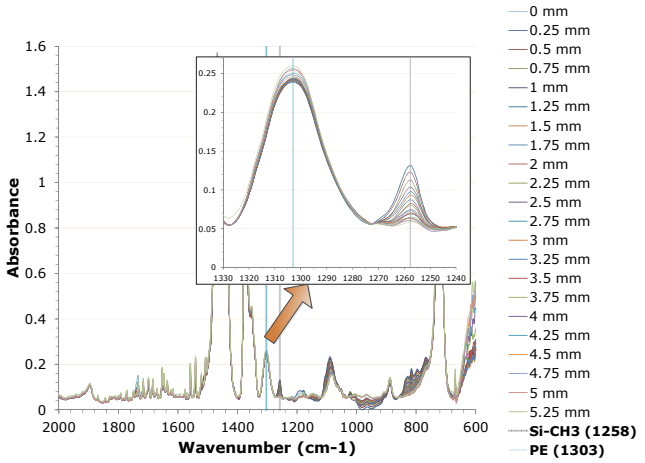

Figure 4. A family of μFTIR spectra from 22 radial locations of exemplary treated cable sample 67.1. The two annotated bands at 1303 and 1258 cm^{-1} are amplified in the inset and are used to quantify silicone concentration in PE.

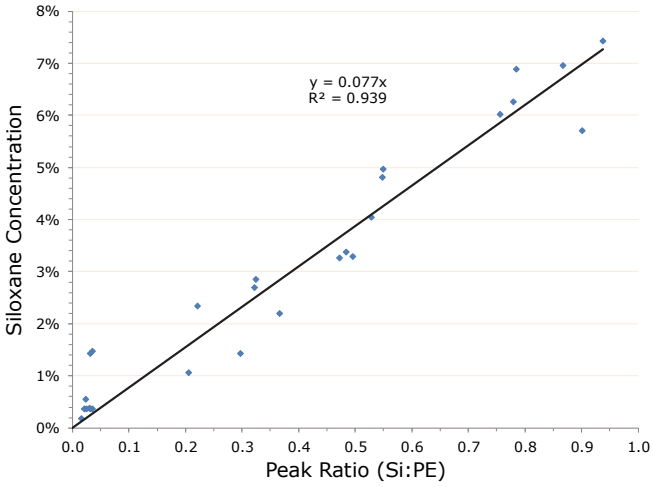

Figure 5. Gravimetric calibration curve fit to 27 data points. About 94% of the variation is explained by Beer's Law. The remaining variation is experimental error.

One further adjustment to this parameter is required. As described in [18], rejuvenation fluid changes from its original injected state, a mixture of alkoxysilane monomers, to its oligomerized siloxane state where the alkoxy portions have been stripped from the original fluid upon reaction with ubiquitous water. It is this siloxane that is found in actual cable samples after even modest aging at an elevated temperature of 55 °C while immersed in a water bath. Stripping the alkoxy portion of the silane serves to concentrate the active portion of the monomeric silanes and this concentration factor can be calculated with reaction stoichiometry. A concentration factor of 0.725 reflects the stoichiometry of the hydrolysis and condensation reactions of the monomer mixture utilized. A single gram of monomer mixture yields about 0.725 g of oligomer. A revised Beer's Law slope corrected for stoichiometry changes is 0.0561 (i.e., the product of 0.0774 and 0.725).

A family of μFTIR spectra, illustrated in Figure 4, is transformed by the gravimetric calibration of Figure 5 and the stoichiometric adjustment to yield a single concentration profile of siloxane oligomer versus a radial distance from the conductor shield. Figure 6 illustrates four such concentration profiles for exemplary cable sample t7-67. Each of the four subsamples labeled with suffixes .1 through .4 are taken from positions across the 12-meter axial length of the sample and from random radial orientations, as illustrated in Figure 3. Three, four or five such concentration profiles were measured for select samples (designated with the Greek character "μ" in Table 1) to ascertain the axial and radial variations of fluid concentration.

Concentration profile sets, exemplified by Figure 6, were obtained for the 19 samples delineated in Table 1 with white boxes. All 19 concentration profile sets are presented in Figures 7, 8, and 9 for the T7, T30, and T90 cohorts, respectively, with consistent Y-axis scaling from 0 to 2.1%$_w$.

To convert these concentration profiles into values that might be correlated to performance, individual values along the insulation radii are integrated within the cylindrical geometry to yield average concentration values. The author

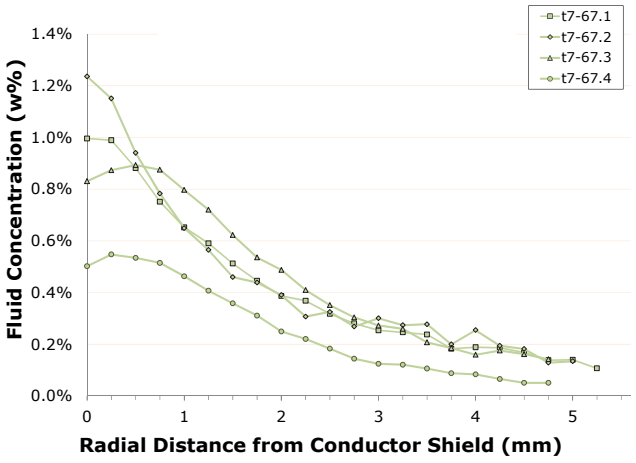

Figure 6. Exemplary set of four radial concentration profiles for sample T7-67. Axial position and radial orientation for each profile are random.

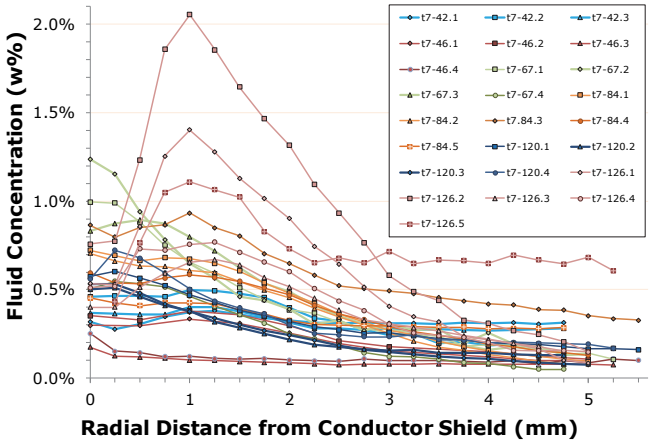

Figure 7. T7 cohort concentration profiles.

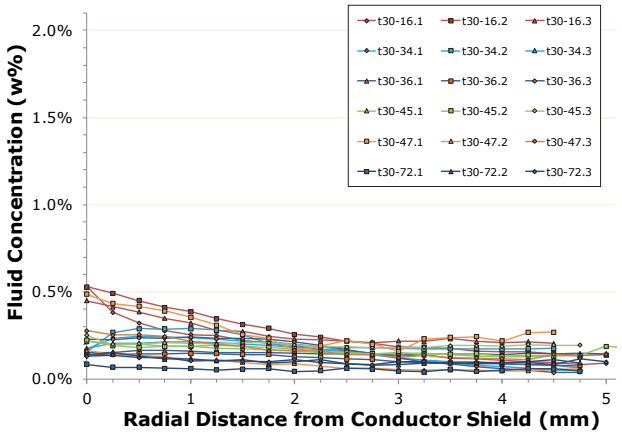

Figure 8. T30 cohort concentration profiles.

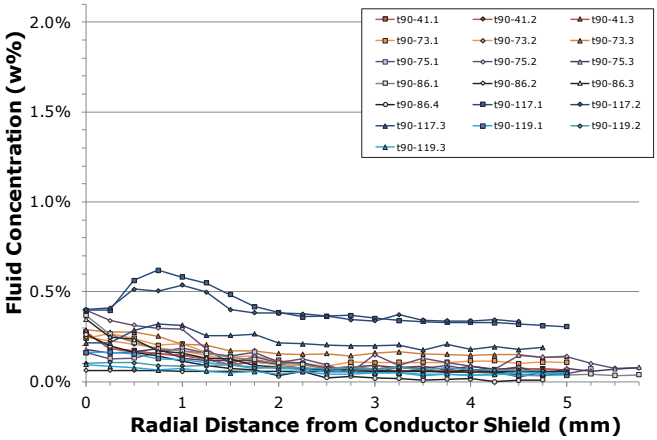

Figure 9. T90 cohort concentration profiles.

examined average values over the insulation radii within their inner third, middle third, outer third, and taken as a whole.

2.3 TESTING

Continuously monitored PD behavior during all ACBD tests (on 42 samples) allowed for the analysis of an extensive amount of time independent and dependent PD characteristics. The assessment and characterization of PD behavior is complex given its stochastic nature and multi-variate dependency on factors, such as:

- Type of defect causing PD (e.g., point discontinuity versus bulk gas-filled void versus interface)
- Location of defect
- Intensity of discharge
- Voltage stress applied
- Temperature, pressure, etc.

PD inception voltage (PDIV) per IEC 60270 refers to the applied voltage at which repetitive partial discharges are first observed in the test object, when the voltage applied to the object is gradually increased from a lower value at which no partial discharges are observed. The primary basis for this type of 'binary' assessment of PD activity is phase resolved PD (PRPD) analysis. This approach allows for analysis of PD activity of 5–10 pC or lower above the background noise

floor, discrimination of internal (cable) dielectric PD from external sources and insight into PD defect physics to separate various types of dielectric PD activity. The PDIV level is defined as the applied voltage step where the PD activity was first observed, not the absolute value during ramp-up stages where external PD activity can distort results. PD activity less than 5 pC was ignored.

3 RESULTS

3.1 MODEL

The Fisher generalized linear model (GLM) as utilized herein is represented by Equation (2). As described in [19, 20] to best fit data with multiple independent variables, the GLM allows the choice of error distributions and the functional form of the relationship between the response and explanatory variables via the link function. Examples of a link function include identity, log, and power. Multiple goodness-of-fit criteria such as AIC (Akaike information criterion) and R-Square are available to quantify and choose the best fit.

$$ln(Y_j) = \beta_{oj} + \beta_{1j}X_1 + \beta_{2j}X_2 + \beta_{3j}X_3 + \varepsilon_j \quad (2)$$

In Equation 2, "j" is one of three dependent variables of interest. The dependent variables are ΔACBD and PDIV. X_1, X_2, and X_3 are independent variables, namely fluid concentration, cable vintage (year manufactured) and transportation impact. The transportation impact is binary: uncompromised cohorts or compromised cohort. Epsilon (ε) is the residual error array.

Both ΔACBD and PDIV were best modeled with Equation (2), by specifying a gamma error distribution. A fourth independent variable, namely the cable manufacturer, was tested in the model. The variable is displayed in column 2 of Table 1 labeled "Mfr." There is a high degree of collinearity between this variable and cable vintage as determined by the Pearson's Chi-squared test. The Chi-squared test indicated a statistically significant collinearity, above a 99.9% confidence level. Overall significance of model results and AIC (Akaike's Information Criterion) suffered with the inclusion of this variable. The cable manufacturer was left out of the model. Eight methods of representing insulation fluid concentration were also tested. The eight methods were composed of four radii ranges each with two compilation approaches. Compilations included average integrated concentration and minimum concentrations over the four radii ranges: overall, inner-third, middle-third, and outer-third. The model results remained essentially similar with all eight representations. The overall minimum fluid concentration was chosen, as it represents the "weaker link" in the cable described in Section 1.4.

Maximum partial discharge at breakdown (MaxPD at BD) resisted all attempts at statistical modeling. Contributing to this challenge were three termination failures, three cases where the cable did not breakdown because its ACBD exceeded the maximum voltage capabilities of the test equipment – about 250 kV, and two failures of equipment to capture a valid MaxPD at BD value. Eight data points and eight degrees of freedom were lost.

3.2 TRANSPORTATION IMPACT

The three regimens (T7, T30, and T90) and control (C) samples fell into three handling-transportation cohorts (C1, C2, and C3). Control (C) and Cohort 1 (C1) samples were shipped from Washington state to Ontario in August, 2017. The C1 samples were rejuvenated and aged at the Ontario laboratory. No post-rejuvenation shipping was required. All T7 samples were included in C1. C2 and C3 samples were treated and aged in Washington and shipped in water filled tubes in September, 2017 and December, 2017, respectively. C2 included six of nine T30 samples. C3 included the remaining three T30 samples and all eight of the T90 samples.

The C3 samples are designated in Figure 4 with white diagonal lines and were compromised during transportation. Those without white diagonal lines (C1 and C2) were uncompromised. Rather than removing compromised values from the analysis and discarding the information those data hold, this variable was modeled with Equation 2. Cables impacted by the transportation issue (C3) suffered a 73% decrease in ΔACBD and a 55% decrease in PDIV. There is greater than a 99.9% chance this parameter is not the result of random variation for both ΔACBD and PDIV. The inclusion of handling-transportation impact improves goodness of fit as indicated by the AIC. In Figures 10–14, samples that did not suffer handling-transportation damage are referred to as "treated (uncompromised)."

The author considered several hypotheses that may have led to the C3 sample damage. The effort to definitively determine the cause would be an exercise with little practical benefit, time consuming, and add little to this work. The results are sufficiently robust with the data collected. The most likely cause of the C3 sample damage was the multiple unintended freeze-thaw cycles experienced during transportation from Washington State to Ontario, Canada. The location and its ambient temperatures as a function of time of the unheated trailer is known and as many as 4 freeze-thaw cycles were experienced. The C3 samples where fully immersed in water-filled flexible PVC tubes and coiled in about 1-meter diameter coils. The change in volume of water upon freezing is about 9% from [21]. If the cable samples had been in straight water-filled tubes, two dimensions of the volumetric expansion would have been harmlessly expended through a diameter increase in the flexible tubing. In a straight tube, elongation would have been about 2.92%. This level of elongation itself will damage a cable, but this analysis underestimates the elongation because the cable was not straight and, hence, up to two of the three Cartesian coordinates were constrained. Actual deformation (elongation and bending) of the cable was between 2.92% and 5.93%.

3.3 CABLE VINTAGE

Cable vintage was determined by printed values on the outer shield whenever those values were available. Where printed values were unavailable, a commercial home valuation web site was used to determine the earliest house construction in the cable's neighborhood. In these cases, cable vintage is assumed to be the date of the earliest house construction. For

each additional year of service, ΔACBD decreases by 7% and PDIV decreases by 4%. There is greater than a 99.9% chance this parameter is not the result of random variation for both ΔACBD and PDIV.

3.4 FLUID CONCENTRATION

3.4.1 ΔACBD

Figure 2 shows the general relationship of fluid concentration and ΔACBD strength of fluids (coded: '841) utilized in the 20th Century. Figure 10 combines the Figure 2 data with data from the present study with a univariate view.

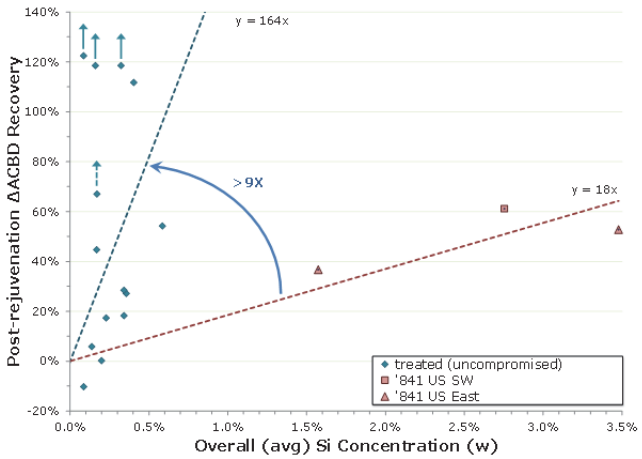

Figure 10. The slope of the 21st Century ΔACBD is at least 9-times steeper than its 20th Century counterpart. Some of the apparent error in this univariate view is explained by cable vintage. The balance of the error reflects measurement uncertainties. The up-arrows on four of the treated points indicate that the actual values lie above the reported values. The sample with a dashed arrow suffered a laboratory termination failure. The other three samples with solid blue arrows reached the maximum voltage of the test equipment.

The slope of the 21st Century ΔACBD is at least 9-times steeper than its 20th Century counterpart. Advanced fluids provide reliable performance at lower concentrations. Low concentration performance is critical for three reasons. First, when cables are near their end-of-life, most susceptible to failure, and initially treated with highly efficacious fluids, dielectric performance will increase more quickly. Before rejuvenation begins fluid concentration is zero. All else being equal, increasing from zero a fluid that is efficacious at low concentrations will provide accelerated reliability improvement compared to a fluid that requires a greater concentration.

Second, geometrically constrained cable as described in [18], particularly 7-strand conductors like those in this study, do not enjoy a large interstitial reservoir. Lower concentrations in these cables are unavoidable. Third, the second law of thermodynamics conspires to decrease fluid concentration with time and hence fluids used to treat cables that function well at low concentrations enjoy longer lives than those that are effective only at higher concentrations. It is for these reasons that a focus on concentrations 3–7 times lower than previous studies is noteworthy.

Solving Equation (2) demonstrates ΔACBD increases 40% for each $0.1\%_w$ minimum fluid concentration increase over the range of $0–0.5\%_w$. There is greater than a 99% chance this parameter is not the result of random variation.

3.4.2 PDIV

Together, Figures 11 and 12 illustrate the improvement of utilizing the minimum silicone concentration as the independent variables, rather than the average. This univariate analysis demonstrates a doubling of the R^2 goodness-of-fit. Using the more robust GLM approach of Equation 2, each incremental $0.1\%_w$ silicone concentration increases PDIV by 21% for the average concentration and 27% for the minimum concentration. There is greater than a 99.9% chance the model outcome is not the result of random variation.

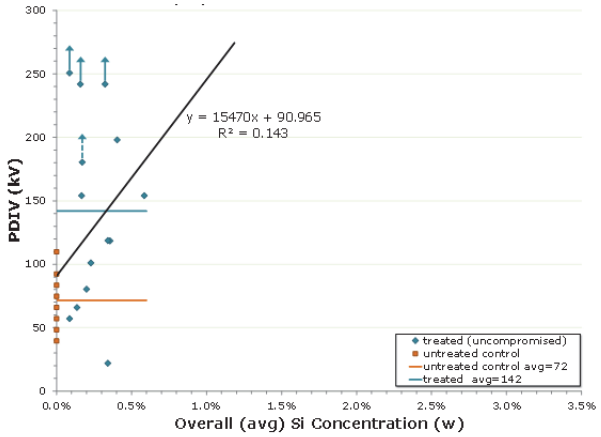

Figure 11. PDIV versus average silicone concentration.

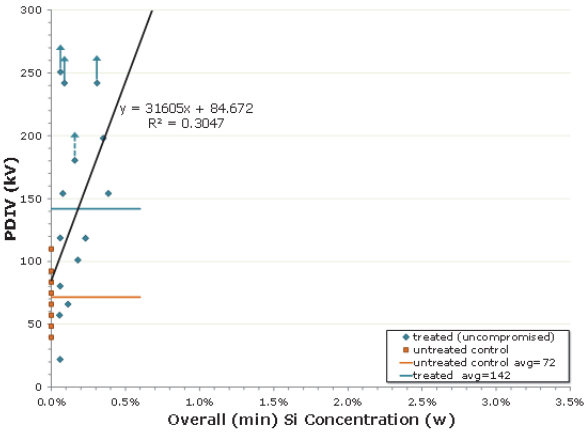

Figure 12. PDIV versus minimum silicone concentration.

3.4.3 CROSS CORRELATION: ΔACBD AND PDIV

As demonstrated in Sections 3.4.1 and 3.4.2, both ΔACBD and PDIV improve as the concentration of rejuvenation fluid increases. Most practitioners of the art of cable dielectrics will not be surprised by this result, however, the authors are unaware of this cross-correlation ever being demonstrated by other researchers. We believe this contribution is the first where PD measurements were made concurrently with ACBD measurements. Figure 13 shows the relationship between

PDIV and ΔACBD. About 94% of the variation between the two variables is correlated. Once PD initiates in unfilled solid dielectrics, the most severe PD site likely progresses rapidly to failure.

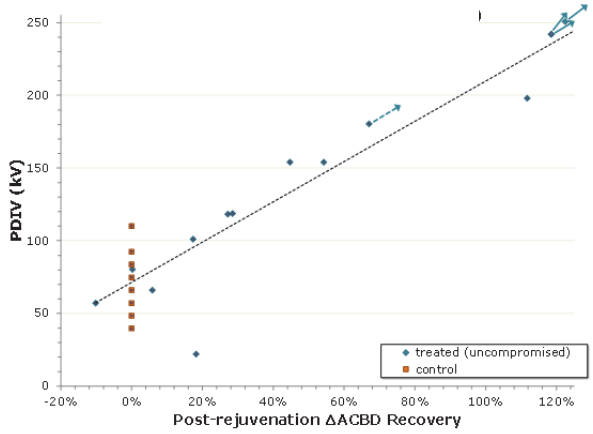

Figure 13. PDIV and ΔACBD are closely cross correlated. As in Figures 10–12, values with blue arrows represent data points with true values greater than those displayed. Here both the x-values and y-values are greater and the result, most likely, is roughly parallel to the slope of the dashed, least squares line. Two of the data points occupy the same x-y coordinate and, hence, two arrows are used to delineate these collocated points.

4 CONCLUSIONS

This contribution reaffirms previous studies demonstrating that the post-treatment ΔACBD performance of cable rejuvenation fluids increases with the concentration of the active ingredients. Chemistry and process advances in the 21st Century have driven nine-fold dielectric performance improvement above 20th Century technology. New generation fluids perform at much lower concentrations than legacy fluids. More effective fluids that operate at lower concentrations yield longer post-rejuvenation life.

All samples in this study were identified by an unaffiliated off-line PD testing firm as "critical" cables, which must be addressed. Rejuvenation addresses the problems in these cables whether those problems are large water trees, gas-filled voids, or electrical trees initiated by testing or other perturbations of voltage above operational levels. For the first time, this work directly demonstrates that partial discharge inception voltage (PDIV) is increased and improved by 27% for each 0.1% increase in fluid concentration in field-aged rejuvenated cables. Gas-filled voids, including electrical trees, are affirmatively addressed with modern rejuvenation fluid. Any PD in joints or terminations are addressed in the sustained pressure rejuvenation (SPR) process, which replaces all terminations and joints. We believe this contribution is the first to establish the correlation between PDIV and ΔACBD.

These results demonstrate that rejuvenation interferes with partial discharge mechanisms by plasticizing the dielectric, filling the voids, smoothing electrical stress, and sequestering free electrons in field-aged cables.

ACKNOWLEDGMENT

G. J. Bertini thanks Sumadhu Arigala (Novinium) who performed the statistical analysis, Westy Ford (Novinium) who managed and executed the sample preparation activity, Dr. Jason McCary (Novinium) who executed the μFTIR work, Dr. Dave Busby (Novinium) who compiled the μFTIR data, and Sarajit Banerjee (Kinectrics) who supervised the AC breakdown and partial discharge work and provided suggestions for the improvement of this contribution.

REFERENCES

[1] F. Steennis, W. Boone, and A. Monfoort, "Water Treeing in Service Aged Cables, Experience and Evaluation Procedure," IEEE Trans. Power Del., vol. 5, no. 1, Jan 1990.
[2] G. Bertini and W. Chatterton, "Dielectric Enhancement Technology," IEEE Electr. Insul. Mag., vol. 10, no.2, pp. 17–22, March/April 1994.
[3] G. Bertini *et al,* "Method for enhancing the dielectrical strength of a cable using a fluid mixture," US Patent 5,372,841, Dec 13, 1994.
[4] S. Mokry *et al,* "Cable fault prevention using dielectric enhancement technology," Jicable 1995.
[5] S. Arigala *et al,* "A Tale of Two Fluids," IEEE, PES, Electrical Insulation Conference, Jun 13, 2017.
[6] G. Bertini *et al*, "Better Next Year: What Rejuvenation Teaches about PD Testing," *ICC SubA,* 2017 (published in fall meeting minutes).
[7] S. A. Boggs, "Partial Discharge: Overview and Signal Generation," IEEE Electr. Insul. Mag., vol. 6, no. 4, pp. 33–39, Jul–Aug 1990.
[8] S. A. Boggs, "Partial discharge. III. Cavity-induced PD in solid dielectrics," IEEE Electr. Insul. Mag., vol. 6, no. 6, pp. 11–16, Nov–Dec 1990.
[9] G. Bertini, "Accelerated Aging of Rejuvenated Cables: Part II," *IEEE PES ICC Sub A,* 2005.
[10] R. M. Hill, *Siloxane surfactants*. In: Robb I.D. (eds) *Specialist Surfactants*. Springer, Dordrecht, 1997. Available: https://doi.org/10.1007/978-94-009-1557-2_6.
[11] G. Mattay and D. Labbé, "Exploring the Water Treeing Inhibition Effect of Antioxidants for XLPE Insulation," IEEE PES ICC, 2006.
[12] Y. Sekii et al, "Effects of Antioxidants on Electrical Tree Generation in XLPE," *IEEE Int. Conf. Solid Dielectrics (ICSD)*, 2001.
[13] H. Sarma, "Water Resistant Electrical Insulation Compositions," US patent 5,719,218, Feb. 17, 1998.
[14] H. Kato *et al,* "Effect and Mechanism of Some New Voltage Stabilizers for Cross-Linked Polyethylene Insulation," *Annu. Rep. Conf. Electr. Insul. Dielectr. Phenom. (CEIDP),* 1974.
[15] J. Wartusch, "Verfahren zur Herstellung von Stabilisierten Vernetzten Formteilen," Patent D 3,014,771, Oct. 1981.
[16] G. Bertini, "System and Method for Predicting Performance of Electrical Power Cables," US patent 7,643,977, Jan. 5, 2010.
[17] B. Fryszczyn, "Full Reel Impregnation of New 15kV XLPE URD Cable," CTL Report 88-068, Aug. 1988.
[18] G. Bertini *et al,* "Balancing Carbons," *IEEE PES ICC,* 2015.
[19] J. Nelder and R. Wedderburn, "Generalized Linear Models," J. R. Stat. Soc. A, vol. 135, pp. 370-384, 1972.
[20] P. McCullagh, J. Nelder, *Generalized Linear Models*, 2nd ed. London: Chapman & Hall; 1989.
[21] M. Kharseh, "Utilize freezing water to generate energy," M. SN aAppl. Sci. (2019) 1: 127. available: HTTPS://DOI.ORG/10.1007/S42452-018-0139-Z.

Glen J. Bertini is the Founder of Novinium, Inc. He has spent over three decades working with technology to extend the life and improve the safety of underground distribution equipment. He has over 60 articles published and holds a total of 34 U.S. patents on cable rejuvenation and explosion prevention with more pending. He holds a B.S. in chemical engineering from Michigan Technological University. He is a Fellow of the IEEE, a Senior member of the ICC, a Senior Member of the AIChE, and a licensed professional engineer in Michigan.

Hunly Chy, P.E., MSEE, MBA, IEEE member, is an Engineering Manager of T&D Linear Asset Engineering at Southern California Edison. He is responsible for the standards development, technical requirement, and strategy as it relates to cable and wire from 600 V to 500 kV. He received his BS and MS of Science in Electrical Engineering from California State University of Los Angeles in 2003 and 2011, respectively. He received his MBA from the University of Laverne in 2014. He is a registered professional engineer in California.